ACS APPLIED MATERIALS & INTERFACES

Research Article

www.acsami.org

Colorless, Transparent, Dye-Doped Polymer Films Exhibiting Tunable Luminescence Color: Controlling the Dual-Color Luminescence of 2-(2′-Hydroxyphenyl)imidazo[1,2-*a*]pyridine Derivatives with the Surrounding Matrix

Shintaro Furukawa, Hideaki Shono, Toshiki Mutai,* and Koji Araki*

Department of Materials and Environmental Science, Institute of Industrial Science, the University of Tokyo, 4-6-1 Komaba, Meguro-ku, Tokyo 153-8505, Japan

Supporting Information

ABSTRACT: Colorless, transparent, polymer films including 2-(2′-hydroxyphenyl)imidazo[1,2-*a*]pyridine (HPIP) derivatives, **1** and **2**, are prepared by a spin-coating method. The observed emission spectra upon photoexcitation of these polymer films were composed of dual emission bands: the normal luminescence at 370−410 nm (purple) and the greatly Stokes-shifted emission at 520−580 nm (yellow) assigned as the excited-state intramolecular proton transfer (ESIPT) luminescence. Relative intensity of the two emissions varied according to the polymer matrices, resulting in change in the luminescent color of the dye-doped polymer films. Particularly, the luminescence properties of 6-cyano HPIP, **2**, are highly susceptible to the surrounding environment, and therefore successfully tuned to produce a wide range of colors, from purple to orange, by changing its concentration within and the type of the polymer matrix. This observation can be ascribed to the formation of a relatively weak intramolecular hydrogen bond resulting from the electron-withdrawing 6-cyano group. Thus, we demonstrate large variations in emission color can be achieved using interactions of the single component with the surrounding matrix. These results offer promise as a convenient and effective method for a wide-range tuning the luminescence colors of dye-doped polymer films.

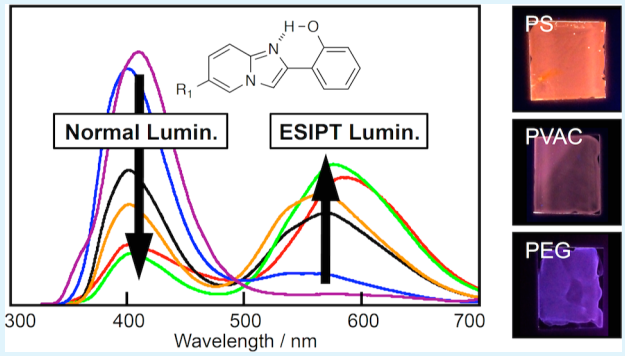

KEYWORDS: *luminescence, fluorescence, dye-doped polymer, transparent film, ESIPT, hydrogen bond*

INTRODUCTION

Solid-state organic materials that exhibit intense luminescence have been attracting considerable interest in various fields.[1−7] Among such materials, those displaying color-tunable emissions[8−16] are especially targeted in order for possible applications such as new types of light sources, photoelectronic materials, and sensor devices. The ability to tune the luminescence properties of these materials by exploiting molecular packing effects, rather than synthetic modifications of chemical structure, has been studied extensively,[15,16] although for the most part, the range of emission colors has been limited. A straightforward and effective way to achieve considerable variation in emission color is to combine materials with differing luminescence bands. This approach has already been applied for most known white-light-luminescent materials using species that exhibit short-wavelength and long-wavelength visible luminescence.[17,18] However, the design of such multicomponent solid-phase systems can be fraught with complications arising from unfavorable resonance energy transfer and intermolecular interactions among other factors.[19]

The above-discussed problems can be circumvented by low-energy emission called the excited-state intramolecular proton transfer (ESIPT) luminescence, which is characterized by a large Stokes shift (~10 000 cm^{-1}). The ESIPT process rapidly occurs after photoexcitation of the intramolecular hydrogen-bonded enol species, then the generated excited-state intramolecular proton-transferred species (IPT*) deactivates with radiation of the ESIPT luminescence (IPT* → IPT) (Scheme 1a).[20−22] In a polar environment, where the intramolecular hydrogen bond is not formed, the dominant "open-enol" species that does not involve proton transfer shows normal luminescence. Park and his group designed a white-light-emitting compound by incorporating two different ESIPT-emitting units within a single molecule.[23] We have previously reported a white-light-emitting solid that combines two compounds displaying normal and ESIPT luminescence, respectively.[24] It has become apparent that integrating normal and ESIPT luminescence is a promising approach for inducing large changes in emission color.

Received: June 22, 2014
Accepted: August 25, 2014
Published: August 25, 2014

Scheme 1. (a) Energy Diagram Illustrating the ESIPT Process, (b) Chemical Structures of 1−3, and (c) Hydrogen-Bonded-Enol (1a, 2a) and Open-Enol (1b, 2b) Forms

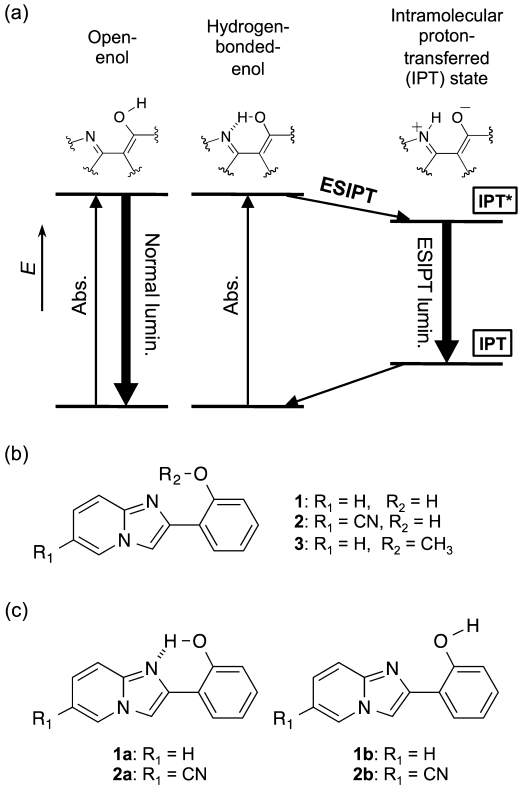

Dual luminescence arises when both the ESIPT process and normal process occur simultaneously within the same material. Hence, we seek to realize large variations in emission color by controlling the dual luminescence of a single luminescent component.

ESIPT luminescence of 2-(2′-hydroxyphenyl)imidazo[1,2-*a*]pyridine (HPIP) was first studied by Acuña and Douhal,[25−27] and that of some derivatives was reported recently by a group of Gryko and Cyrański.[28] Our group reported bright ESIPT luminescence in the solid state.[29−31]

In this study, we show that relative intensity of the normal and ESIPT emissions from HPIP derivatives, **1** and **2** (Scheme 1b), within spin-coated polymer films can be tuned by altering the surrounding matrices, resulting in a wide range of luminescence colors.

EXPERIMENTAL SECTION

Materials. HPIP (**1**),[29] 6-cyano HPIP (**2**),[30] and the methoxy-containing derivative (**3**)[29] (Scheme 1b) were prepared according to the previously reported method. The following commercially available polymer/solvent sets were then used for spin-coating: polystyrene (PS, Aldrich, M_w ~230 000)/$CHCl_3$, poly(vinyl acetate) (PVAC, Kanto, M_w ~170 000)/$CHCl_3$, poly(bisphenol A carbonate) (PC, Aldrich, M_w ~45 000)/$CHCl_3$, poly(methyl methacryrate) (PMMA, Aldrich, M_w ~120 000)/$CHCl_3$, poly(vinyl alcohol) (PVA, Aldrich, 80% hydrolyzed, M_w 9000−10 000)/ethanol−water (70 v/v%), and poly(ethylene glycol) (PEG, Fluka, M_w ~35 000)/ethanol. Quartz plates (15 × 15 × 1 mm) were obtained commercially and rinsed with ethanol in an ultrasonic bath for 10 min before use.

Methods. Spin-coated films were prepared with a Mikasa MS-A100 spin coater. A drop of polymer solutions (100 g dm^{-3}) containing either HPIP (**1**) or 6-cyano HPIP (**2**; 0.5 w/w% with respect to polymer) were spin-coated at 1000 rpm onto quartz plates and then dried in a vacuum at 80 °C for 12 h. Dilute PVA solutions (5.0 g dm^{-3} in 70 v/v% ethanol/water) containing higher concentrations of **2** (2, 5, 10, and 30 w/w% with respect to PVA) were spin-coated for preparing films with higher content of **2** (thickness: ~0.1 μm).

Luminescence spectra of polymer films were recorded on a JASCO FP-6600 spectrofluorophotometer equipped with an ILF-533 integral sphere, and the quantum yields were calculated with a built-in software based on a literature method.[32] IR spectra were measured on a JEOL WINSPEC100 spectrophotometer. Quantum chemical properties of the enol and intramolecular proton-transferred (IPT) species of **1** and **2** were calculated by density functional theory (DFT) after geometry optimization using B3LYP/6-311++G(d,p) basis set. The calculation job files are presented in Supporting Information. These calculations were performed with a Gaussian 09W, Gaussian Inc. (Revision D.01).[33]

RESULTS AND DISCUSSION

Matrix-Induced Color Tuning of Luminescence. Smooth, colorless, transparent films of various polymers containing **1** and **2** (0.5 w/w%) were successfully spin-coated onto quartz substrates. Upon UV-light irradiation, films containing **1** showed green to yellow-green luminescence, and those of **2** produced a variety of luminescent colors such as purple, yellow, and orange. As shown in Figure 1, emission spectra of **1** and **2** held within these polymer films were composed of dual emission bands at around 370−410 nm and 520−580 nm.

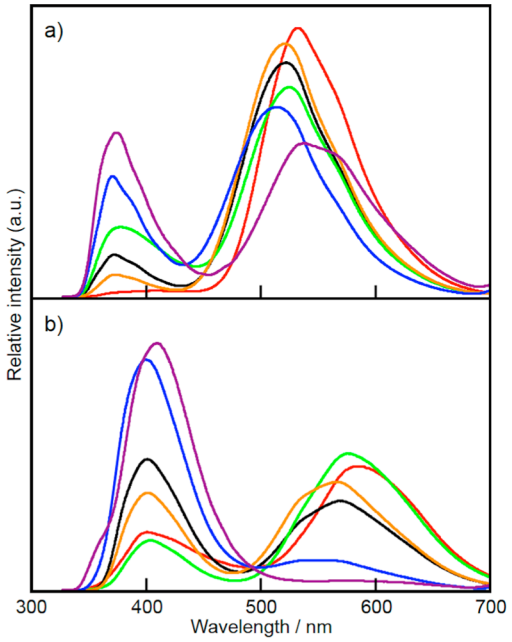

Figure 1. Emission spectra (λ_{ex} = 333 nm) of spin-coated films containing 0.5 w/w% of **1** (a) and **2** (b) in PS (red) PVAC (black), PC (green), PMMA (orange), PVA (blue), and PEG (purple). Emission intensities are normalized with respect to quantum yield.

We previously reported that **1**[29] and **2**[31] exhibit polymorph-dependent luminescence as their differing crystal structures cause them to luminesce with different colors. The emission spectra of the polymorphic crystals are composed of only a single, largely Stokes-shifted band at around 500−600 nm, assigned as ESIPT luminescence from IPT* species generated by excitation of the hydrogen-bonded-enol species (**1a** and **2a**, Scheme 1c).[30] On the other hand, **1** shows a weak normal emission band at around 370 nm in a protic solution, which is

attributed to the species not engaged in an intramolecular hydrogen bond in the ground state (open-enol form; **1b**).[30] The protic solvent encourages dissociation of the intramolecular hydrogen bond within **1a** to produce **1b**. Therefore, two distinct emission bands of the polymer films are assignable to normal and ESIPT luminescence from open-enol (**1b** and **2b**) and hydrogen-bonded species (**1a** and **2a**), respectively.

To confirm the above assignment, the luminescence properties of **1** in PMMA film (0.5 w/w%) were compared with those of the two crystalline polymorphs,[29] **1** in a dilute ethanol solution, and methoxy derivative **3** (intrinsically unable to form an intramolecular hydrogen bond) in PMMA film (Figure S1, Table 1). As for the lower-energy emission band of

Table 1. Photophysical Properties of HPIP Derivatives 1 and 3

	compound	λ_{em}/nm		Φ	τ/ns
1	crystal[a] polymorph I		496	0.50	5.61
	polymorph II		529	0.37	5.84
	PMMA film (0.5 w/w%)	377		0.40	–[b]
			523		4.89
	ethanol solution	377		0.10	0.99
	cyclohexane solution		570	0.03	1.67
3	PMMA film (0.5 w/w%)	382		0.30	2.84

[a]Ref 29. [b]Not measured.

1 in PMMA film observed at around 550 nm, the characteristically large Stokes shift and nanosecond-order lifetime were similar to those of the polymorphic crystals. On the other hand, the higher-energy emission at around 380 nm was also observed for **1** in ethanol solution, and for **3** in a PMMA film. It can therefore be concluded that the higher-energy emission band is due to normal emission from **1b** (open-enol form), and that the lower-energy emission band is due to ESIPT luminescence from the intramolecularly hydrogen-bonded form (**1a**) via IPT*. Thus, the two emission bands produced by **1** and **2** are attributable to coexisting forms within each sample.

We then examined an opposite shift of the ESIPT luminescence of **1** observed in polar matrices: blue shift in PVA and red shift in PEG. As proposed in Figure S2a,b (Supporting Information), both matrices and the emitting species of **1** can be hydrogen-bonded, but in different modes. In PVA, a hydrogen bond could be formed between alcoholic hydrogen and oxygen of **1** (Figure S2a, Supporting Information), whereas in PEG, a hydrogen bond could be formed between N–H hydrogen of **1** and oxygen of PEG (Figure S2b, Supporting Information). Meanwhile, computational simulation on the ESIPT luminescence indicates that the electron density of IPT* is localized on the imidazo[1,2-*a*]pyridine unit, whereas that of IPT is localized on the phenoxy unit (Figure S2c,d, Supporting Information). Therefore, in PVA, the proposed hydrogen bond formation would result in lowering the energy level of IPT by somewhat neutralizing the high electron density on the phenoxy unit, but would be hardly effective on the energy level of IPT* because of deficient electron density on the phenoxy unit. Thus, the ESIPT emission energy (IPT* → IPT) gets larger, i.e., blue shift. On the basis of the similar discussion, hydrogen bonding to N–H would lower the energy level of IPT*, but not that of IPT, resulting in smaller emission energy in PEG.

The CIE 1931 chromaticity diagram of the luminescing polymer films is shown in Figure 2. Whereas the *x*,*y* coordinate

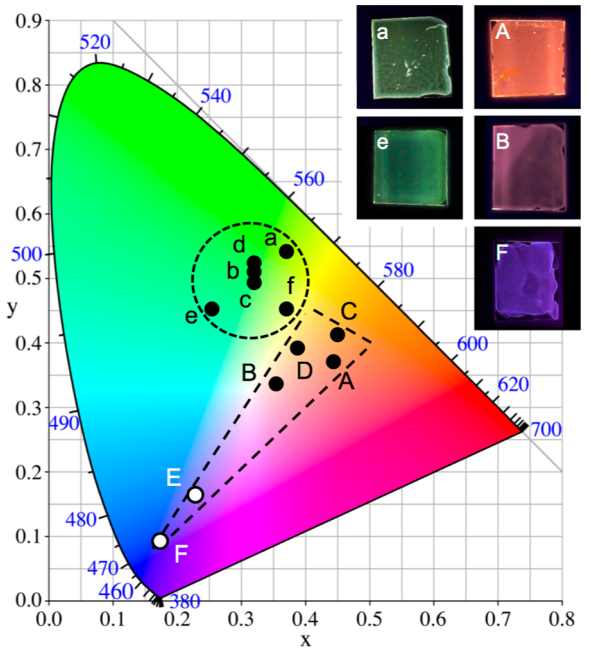

Figure 2. CIE 1931 chromaticity diagram of the luminescence (λ_{ex} = 330 nm) of spin-coated films containing 0.5 w/w% of **1** (a–f) and **2** (A–F) in PS (a, A) PVAC (b, B), PC (c, C), PMMA (d, D), PVA (e, E), and PEG (f, F). Images in the upper right corner show polymer films luminescing under a UV lamp (365 nm).

of **1** in various matrices was similar, those of **2** depended greatly on the nature of the polymer matrix. To understand such large color variation, the effect of matrix composition on the maximum emission wavelength (λ_{em}) and the normal/ESIPT emission intensity ratio (I_N/I_E) was examined. As shown in Table 2, the λ_{em} values of both normal (N) and ESIPT (E) luminescence bands of **1** and **2** were not greatly affected by the matrices. The normal luminescence maxima appeared within a range of 10 nm, indicating practically no change in the emission color. Though the ESIPT luminescence band was slightly more susceptible to the polymer matrix, the change in λ_{em} does not explain the apparently large change of emission color.

On the other hand, the I_N/I_E intensity ratio of **2** varied greatly with the polymer matrix. The relative intensities of normal emissions brought about by polar polymers, such as PVA and PEG, were considerably higher than those induced by nonpolar polymers. Therefore, the large change in the observed emission color of **2** is ascribed to the alteration of I_N/I_E rather than a shift in the λ_{em} of these bands. Because normal and ESIPT emissions originate from **2b** and **2a**, respectively, the polymer matrix appears to have a large effect on the relative abundance of these species. In polar polymer matrices having hydrogen-bond donor and/or acceptor groups, hydrogen bonding with surrounding matrix might be facilitated, resulting to decreased abundance of **2a**.

The matrix-induced change in emission color was much larger for cyano-substituted **2** than it was for **1**. The effect of substitution on the photophysical properties of these HPIP derivatives was analyzed previously by an ab initio quantum chemical method.[30] The report attributed the red-shifted

Table 2. Photophysical Properties of 1 and 2 in Polymer Matrices

compound			1				2				
			λ_{em}/nm					λ_{em}/nm			
polymer	ε[a]	λ_{abs} (nm)	N[b]	E[c]	I_N/I_E[d]	Φ	λ_{abs} (nm)	N[b]	E[c]	I_N/I_E[d]	Φ
PS	2.5	336		534	0.02	0.30	359	404	585	0.47	0.05
PVAC	2.9	330	375	524	0.30	0.30	346	404	571	1.47	0.07
PC	3.2	333	381	527	0.33	0.31	352	407	578	0.37	0.05
PMMA	3.9	332	377	523	0.09	0.40	351	404	569	0.90	0.10
PVA	10	331	373	517	0.62	0.38	346	402	540	7.65	0.10
PEG		332	376	540	1.07	0.23	347	414	574	23	0.04

[a]Dielectric constant of polymer (ref 34). [b]Normal emission. [c]ESIPT emission. [d]Intensity ratio of the normal (I_N) to ESIPT (I_E) emissions at their maximum wavelengths.

ESIPT emission of **2** to the decreased HOMO−LUMO gap in the proton-transferred species (Scheme 1a).

The remarkable susceptibility of **2** to its surrounding polymer matrix cannot be explained directly from the above analysis. We therefore measured IR spectra of powder samples of **1** and **2**, and found their OH stretching peaks (ν_{O-H}) at 3132 and 3137 cm^{-1}, respectively (Figure S3, Supporting Information). Because both compounds predominantly exist as the intramolecularly hydrogen-bonded forms (**1a** and **2a**) in the crystalline and amorphous solid, the higher wavenumber stretching frequency (ν_{O-H}) of **2** indicates that its intramolecular hydrogen bond is weaker than that of **1**. Density functional theory (DFT) calculations (B3LYP/6-311++G-(d,p)) show that the ground state total negative charge on nitrogen at 1-position of **2** (−0.124) is slightly smaller than that within **1** (−0.134), probably due to the electron-withdrawing nature of the 6-cyano substituent in the former. The imidazole nitrogen of **2** is therefore suspected to be a weaker hydrogen-bond acceptor than that of **1**, which would explain the dramatic effect of different polymer matrices on the luminescence properties of **2**, especially when comparing the effects of polar (PVA and PEG) versus nonpolar polymers.

Concentration-Dependent Color Tuning of Luminescence within PVA Films. In both crystalline and amorphous solids composed of a single substance, wherein each molecule is surrounded by others just like it, **2**, which exists exclusively as **2a**, exhibits yellow ESIPT luminescence. On the other hand, a sample containing 0.5 w/w% **2** in a polar PVA matrix displayed a dominant normal emission, indicating that in this case most of **2** exists as **2b**. Therefore, the relative intensity of the two emission bands (I_N/I_E) can also be tuned by varying the concentration of **2** in PVA. Because of the low solubility of **2** in 70 v/v% ethanol/water, a diluted PVA solution (5.0 g dm^{-3}) was used for preparation of the spin-coated films containing 2, 5, 10, and 30 w/w% of **2** with respect to PVA. The thin films prepared on quartz plates were transparent and colorless. Increasing the concentration of **2** (>50 w/w%) resulted in opaque films due to the heterogeneous dispersal of **2**. The thickness of these films was approximately 0.1 μm, which was less than 10% of the thickness of those prepared from the dense PVA solution (100 g dm^{-3}). Figure 3 shows the luminescence spectra of the prepared PVA films. As the concentration of **2** increased, the normal emission gradually decreased with concomitant intensification of the ESIPT emission (Table 3).

As shown in Figure 4, increasing the concentration of **2** within the film induced a change of emission color from purple to white to green. As indicated by the linearity of the plotted color indices in the chromaticity diagram, the observed emission color change was due to alteration of the relative intensities of the normal and the ESIPT emission bands. Thus, higher concentrations of **2** diminished the effect of the polar PVA matrix, because of the increased abundance of ESIPT-emitting **2a** relative to normal-emitting **2b**.

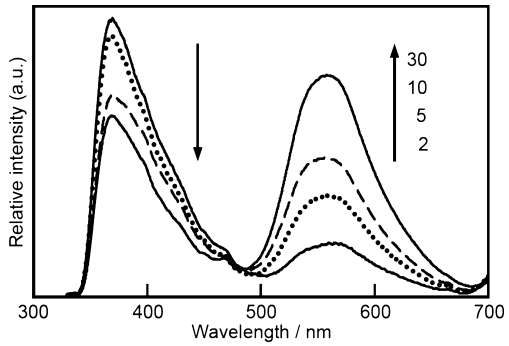

Figure 3. Emission spectra (λ_{ex} = 333 nm) of the spin-coated PVA films containing different amounts of **2** (2−30 w/w%). Emission intensities were normalized with respect to their absorbances at 333 nm.

Table 3. Relative Intensities of the Normal (I_N) to ESIPT (I_E) Emissions As a Function of Concentration of 2 within PVA Films

run	2 in PVA (w/w%)	I_N/I_E[a]	Φ
1[b]	0.5	7.65	0.10
2[c]	2	5.13	–[d]
3[c]	5	2.56	0.13
4[c]	10	1.44	0.21
5[c]	30	0.82	0.24

[a]Calculated at peak maxima. [b]Prepared from a concentrated polymer solution (100 g dm^{-3}) because the emission observed from a film prepared from a dilute polymer solution exhibited poor signal-to-noise. [c]Prepared from dilute polymer solutions (5 g dm^{-3}). [d]Not determined because of the low emission intensity.

CONCLUSIONS

HPIP derivatives, **1** and **2**, within spin-coated polymer films exhibit dual luminescence composed of the normal and ESIPT emissions. The purple normal luminescence band is produced by the open-enol form, **1b** and **2b**, whereas the greatly Stokes-shifted yellow ESIPT luminescence band resulted from the intramolecular hydrogen-bonded enol form, **1a** and **2a**, via the IPT* state. By altering the surrounding matrices, relative intensity of the two emissions can be tuned as a result of change in the abundance ratio of the two enol forms. We

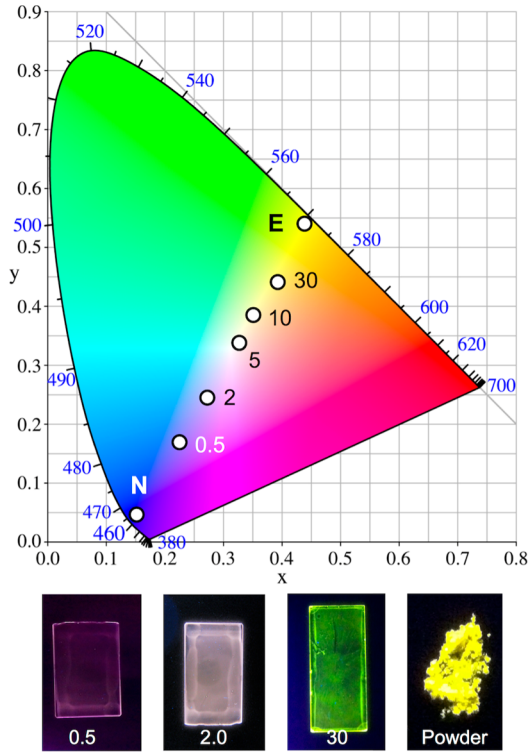

Figure 4. CIE 1931 chromaticity diagram of the luminescence (λ_{ex} = 333 nm) of spin-coated PVA films containing 0.5–30 w/w% of **2**. "N" and "E" represent the color indices of the normal and ESIPT emission bands, respectively. The images below show luminescence of the polymer films and the powder of **2** under a UV lamp (365 nm).

particularly demonstrate how the luminescence of **2** within spin-coated polymer films can be tuned to produce a wide range of colors, from purple to orange, by changing its concentration within and the type of the polymer matrix. The luminescence properties of **2** were highly susceptible to the surrounding matrix, an observation ascribed to the formation of a relatively weak intramolecular hydrogen bond resulting from the electron-withdrawing 6-cyano group. These results demonstrate that the polarity of the surrounding matrix controls the relative intensities of the emission bands produced by normal and ESIPT luminescence processes.

Transparent polymer films have various uses, such as optical materials and surface coating. We therefore think that the results presented here would offer a promising system that can effectively and conveniently control the luminescence color of dye-doped polymer films.

■ ASSOCIATED CONTENT

Ⓢ Supporting Information

Emission spectra of **1** and **3** in organic solutions and crystalline materials, infrared spectra of **1** and **2**, and the job files of the DFT calculation. This material is available free of charge via the Internet at http://pubs.acs.org.

■ AUTHOR INFORMATION

Corresponding Authors

*K. Araki. E-mail: araki@iis.u-tokyo.ac.jp.
*T. Mutai. E-mail: mutai@iis.u-tokyo.ac.jp.

Notes

The authors declare no competing financial interest.

■ ACKNOWLEDGMENTS

The study is partly supported by Grants-in-Aid for Scientific Research (21350109, 24550222 and 23656423) from the Japan Society for the Promotion of Science (JSPS) and Promotion of Scientific Research (0241027-A) from the Iketani Science and Technology Foundation, Japan.

■ ABBREVIATIONS

ESIPT, excited-state intramolecular proton transfer
HPIP, 2-(2′-hydroxyphenyl)imidazo[1,2-*a*]pyridine

■ REFERENCES

(1) Sasabe, H.; Kido, J. Multifunctional Materials in High-Performance OLEDs: Challenges for Solid-State Lighting. *Chem. Mater.* **2011**, *23*, 621–630.
(2) Mishra, A.; Bauerle, P. Small Molecule Organic Semiconductors on the Move: Promises for Future Solar Energy Technology. *Angew. Chem., Int. Ed.* **2012**, *51*, 2020–2067.
(3) Yanai, N.; Kitayama, K.; Hijikata, Y.; Sato, H.; Matsuda, R.; Kubota, Y.; Takata, M.; Mizuno, M.; Uemura, T.; Kitagawa, S. Gas Detection by Structural Variations or Fluorescent Guest Molecules in a Flexible Porous Coordination Polymer. *Nat. Mater.* **2011**, *10*, 787–793.
(4) Zhao, Y. S.; Fu, H.; Peng, A.; Ma, Y.; Liao, Q.; Yao, J. Construction and Optoelectronic Properties of Organic One-Dimensional Nanostructures. *Acc. Chem. Res.* **2010**, *43*, 409–418.
(5) Qian, G.; Wang, Z. Y. Near-Infrared Organic Compounds and Emerging Applications. *Chem.—Asian J.* **2010**, *5*, 1006–1029.
(6) Kamtekar, K. T.; Monkman, A. P.; Bryce, M. R. Recent Advances in White Organic Light-Emitting Materials and Devices (WOLEDs). *Adv. Mater.* **2010**, *22*, 572–582.
(7) Samuel, I. D. W.; Turnbull, G. A. Organic Semiconductor Lasers. *Chem. Rev.* **2007**, *107*, 1272–1295.
(8) Chi, Z. G.; Zhang, X. Q.; Xu, B. J.; Zhou, X.; Ma, C. P.; Zhang, Y.; Liu, S. W.; Xu, J. R. Recent Advances in Organic Mechanofluorochromic Materials. *Chem. Soc. Rev.* **2012**, *41*, 3878–3896.
(9) Hong, Y.; Lama, J. W. Y.; Tang, B.-Z. Aggregation-Induced Emission. *Chem. Soc. Rev.* **2011**, *40*, 5361–5388.
(10) Gierschner, J.; Park, S. Y. Luminescent Distyrylbenzenes: Tailoring Molecular Structure and Crystalline Morphology. *J. Mater. Chem. C* **2013**, *1*, 5818–5832.
(11) Sagara, Y.; Kato, T. Mechanically Induced Luminescence Changes in Molecular Assemblies. *Nat. Chem.* **2009**, *1*, 605–610.
(12) Li, Z.; Dong, Y. Q.; Lam, J. W. Y.; Sun, J. X.; Qin, A. J.; Haeussler, M.; Dong, Y. P.; Sung, H. H. Y.; Williams, I. D.; Kwok, H. S.; Tang, B. Z. Functionalized Siloles: Versatile Synthesis, Aggregation-Induced Emission, and Sensory and Device Applications. *Adv. Funct. Mater.* **2009**, *19*, 905–917.
(13) Mutai, T.; Satou, H.; Araki, K. Reproducible On–Off Switching of Solid-State Luminescence by Controlling Molecular Packing Through Heat-Mode Interconversion. *Nat. Mater.* **2005**, *4*, 685–687.
(14) Luo, J.; Xie, Z.; Lam, J. W. Y.; Cheng, L.; Chen, H.; Qiu, C.; Kwok, H.-S.; Zhan, X.; Liu, Y.; Zhu, D.; Tang, B.-Z. Aggregation-Induced Emission of 1-Methyl-1,2,3,4,5-pentaphenylsilole. *Chem. Commun.* **2001**, 1740–1741.
(15) Varughese, S. Non-Covalent Routes to Tune the Optical Properties of Molecular Materials. *J. Mater. Chem. C* **2014**, *2*, 3499–3516.
(16) Yan, D.; Evans, D. G. Molecular Crystalline Materials with Tunable Luminescent Properties: from Polymorphs to Multi-Component Solids. *Mater. Horiz.* **2014**, *1*, 46–57.
(17) Farinola, G. M.; Ragni, R. Electroluminescent Materials for White Organic Light Emitting Diodes. *Chem. Soc. Rev.* **2011**, *40*, 3467–3482.
(18) Sun, Y. R.; Giebink, N. C.; Kanno, H.; Ma, B. W.; Thompson, M.; Forrest, S. R. Management of Singlet and Triplet Excitons for

Efficient White Organic Light-Emitting Devices. *Nature* **2006**, *440*, 908−912.
(19) Turro, N. J. *Modern Molecular Photochemistry*, 2nd ed; University Science Books: Sausalito, CA, 1991.
(20) Barbatti, M.; Aquino, A. J. A.; Lischka, H.; Schriever, C.; Lochbrunner, S.; Riedle, E. Ultrafast Internal Conversion Pathway and Mechanism in 2-(2′-Hydroxyphenyl)benzothiazole: A Case Study for Excited-State Intramolecular Proton Transfer Systems. *Phys. Chem. Chem. Phys.* **2009**, *11*, 1406−1415.
(21) Lochbrunner, S.; Schultz, T.; Schmitt, M.; Shaffer, J. P.; Zgierski, M. Z.; Stolow, A. Dynamics of Excited-State Proton Transfer Systems via Time-Resolved Photoelectron Spectroscopy. *J. Chem. Phys.* **2001**, *114*, 2519−2522.
(22) Ormson, S. M.; Brown, R. G. Excited State Intramolecular Proton Transfer Part 1: ESIPT to Nitrogen. *Prog. React. Kinet.* **1994**, *19*, 45−91.
(23) Park, S.; Kwon, J. E.; Kim, S. H.; Seo, J.; Chung, K.; Park, S.-Y.; Jang, D.-J.; Medina, B. M.; Gierschner, J.; Park, S. Y. A White-Light-Emitting Molecule: Frustrated Energy Transfer between Constituent Emitting Centers. *J. Am. Chem. Soc.* **2009**, *131*, 14043−14049.
(24) Shono, H.; Ohkawa, T.; Tomoda, H.; Mutai, T.; Araki, K. Fabrication of Colorless Organic Materials Exhibiting White Luminescence Using Normal and Excited-State Intramolecular Proton Transfer Processes. *ACS Appl. Mater. Interfaces* **2011**, *3*, 654−657.
(25) Douhal, A.; Amat-Guerri, F.; Acuña, A. U. Photoinduced Intramolecular Proton Transfer and Charge Redistribution in Imidazopyridines. *J. Phys. Chem.* **1995**, *99*, 76−80.
(26) Douhal, A.; Amat-Guerri, F.; Acuña, A. U. Probing Nanocavities with Proton-Transfer Fluorescence. *Angew. Chem., Int. Ed.* **1997**, *36*, 1514−1516.
(27) Douhal, A. The Involvement of Rotational Processes in the Intramolecular Proton-Transfer Cycle. *Ber. Bunsenges. Phys. Chem.* **1998**, *102*, 448−451.
(28) Stasyuk, A. J.; Banasiewicz, M.; Cyrański, M. K.; Gryko, D. T. Imidazo[1,2-*a*]pyridines Susceptible to Excited State Intramolecular Proton Transfer: One-Pot Synthesis via an Ortoleva-King Reaction. *J. Org. Chem.* **2012**, *77*, 5552−5558.
(29) Mutai, T.; Tomoda, H.; Ohkawa, T.; Yabe, Y.; Araki, K. Switching of Polymorph-Dependent ESIPT Luminescence of an Imidazo[1,2-*a*]pyridine Derivative. *Angew. Chem., Int. Ed.* **2008**, *47*, 9522−9524.
(30) Mutai, T.; Sawatani, H.; Shida, T.; Shono, H.; Araki, K. Rational Approach to Tuning of Efficient Excited-State Intramolecular Proton Transfer (ESIPT) Fluorescence of Imidazo[1,2-*a*]pyridine in Rigid Matrices by Substituent Groups. *J. Org. Chem.* **2013**, *78*, 2482−2489.
(31) Mutai, T.; Shono, H.; Shigemitsu, Y.; Araki, K. Three-Color Polymorph-Dependent Luminescence: Crystallographic Analysis and Theoretical Study on Excited-State Intramolecular Proton Transfer (ESIPT) Luminescence of Cyano-Substituted Imidazo[1,2-*a*]pyridine. *CrystEngComm* **2014**, *16*, 3890−3895.
(32) De Mello, J. C.; Wittmann, H. F.; Friend, R. H. An Improved Experimental Determination of External Photoluminescence Quantum Efficiency. *Adv. Mater.* **1997**, *9*, 230−232.
(33) Frisch, M. J.; Trucks, G. W.; Schlegel, H. B.; Scuseria, G. E.; Robb, M. A.; Cheeseman, J. R.; Scalmani, G.; Barone, V.; Mennucci, B.; Petersson, G. A.; Nakatsuji, H.; Caricato, M.; Li, X.; Hratchian, H. P.; Izmaylov, A. F.; Bloino, J.; Zheng, G.; Sonnenberg, J. L.; Hada, M.; Ehara, M.; Toyota, K.; Fukuda, R.; Hasegawa, J.; Ishida, M.; Nakajima, T.; Honda, Y.; Kitao, O.; Nakai, H.; Vreven, T.; Montgomery, J. A., Jr.; Peralta, J. E.; Ogliaro, F.; Bearpark, M.; Heyd, J. J.; Brothers, E.; Kudin, K. N.; Staroverov, V. N.; Kobayashi, R.; Normand, J.; Raghavachari, K.; Rendell, A.; Burant, J. C.; Iyengar, S. S.; Tomasi, J.; Cossi, M.; Rega, N.; Millam, N. J.; Klene, M.; Knox, J. E.; Cross, J. B.; Bakken, V.; Adamo, C.; Jaramillo, J.; Gomperts, R.; Stratmann, R. E.; Yazyev, O.; Austin, A. J.; Cammi, R.; Pomelli, C.; Ochterski, J. W.; Martin, R. L.; Morokuma, K.; Zakrzewski, V. G.; Voth, G. A.; Salvador, P.; Dannenberg, J. J.; Dapprich, S.; Daniels, A. D.; Farkas, Ö.; Foresman, J. B.; Ortiz, J. V.; Cioslowski, J.; Fox, D. J. *Gaussian 09*, Revision D.01; Gaussian, Inc.: Wallingford, CT, 2009.
(34) Altmann, R. B.; Renge, I.; Kador, L.; Haarer, D. Dipole Moment Differences of Nonpolar Dyes in Polymeric Matrices: Stark Effect and Photochemical Hole Burning. I. *J. Chem. Phys.* **1992**, *97*, 5316−5322.